LBL-9297 Rev.
Preprint c.2

Lawrence Berkeley Laboratory
UNIVERSITY OF CALIFORNIA

ENERGY & ENVIRONMENT DIVISION

Submitted to Passive/Hybrid Journal

NATURAL CONVECTION IN PASSIVE SOLAR BUILDINGS: EXPERIMENTS, ANALYSIS AND RESULTS

Ashok Gadgil, Fred Bauman, and Ronald Kammerud

April 1981

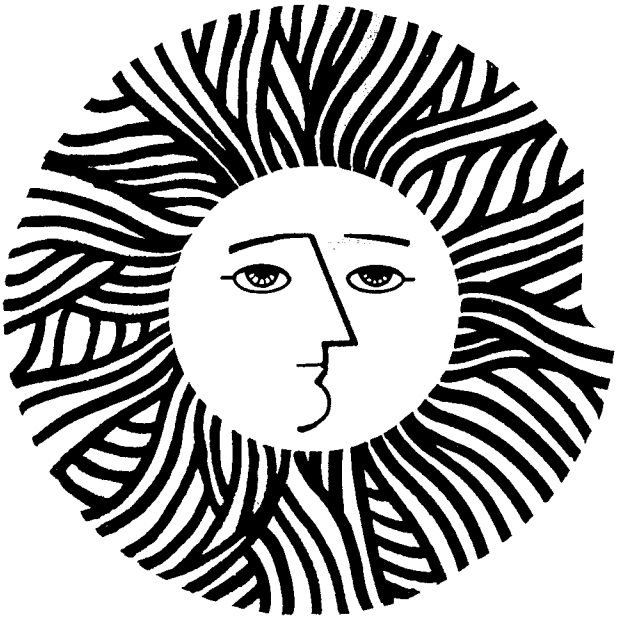

Prepared for the U.S. Department of Energy under Contract W-7405-ENG-48

LBL-9297 (Revised)
April 1981

NATURAL CONVECTION IN PASSIVE SOLAR BUILDINGS: EXPERIMENTS, ANALYSIS AND RESULTS*

Ashok Gadgil, Fred Bauman, and Ronald Kammerud
Passive Analysis and Design Group
Lawrence Berkeley Laboratory
University of California
Berkeley, California 94720

ABSTRACT

Computer programs have been developed to numerically simulate natural convection in two- and three-dimensional room geometries. The programs have been validated using published data from the literature, results from a full-scale experiment performed at the Massachusetts Institute of Technology, and results from a small-scale experiment performed at LBL. One of the computer programs has been used to study the influence of natural convection on the thermal performance of a single zone in a direct-gain passive solar building. It is found that the convective heat transfer coefficients between the air and the enclosure surfaces can be substantially different from the values assumed in the standard building energy analysis methods, and can exhibit significant variations across a given surface. This study implies that the building heating loads calculated by standard building energy analysis methods may have substantial errors as a result of their use of common assumptions regarding the convection processes which occur in an enclosure.

1. INTRODUCTION

In spite of the fundamental role played by natural convection in both conventional buildings and passive solar systems, it has received relatively little experimental or analytic attention within the building sciences. Within a single thermal zone,[+] natural convection and thermal radiation are jointly responsible for the distribution of heat from collection and/or storage media to the building occupants, the occupied space, or to building elements with significant thermal mass which do not receive direct sunlight. In general, several thermal zones are needed to characterize occupied buildings (e.g., buildings other than warehouses, airplane-hangers, etc.); and convection processes contribute to the thermal transfers among these zones. Buoyancy-driven[+] convection is responsible for the air circulation producing a cooling effect in sunspaces, multi-story atria, and in other thermal chimney designs; and finally, many passive solar concepts such as double envelope structures, thermocirculation systems, thermal storage systems using buoyancy-driven air for heat transport, rely almost exclusively on natural convection for their operation.

Recent research results have emphasized the importance of natural convection processes. Analyses performed by the Los Alamos Scientific Laboratory on the Balcomb house [1] have implied the importance of convective coupling of thermal zones as compared to radiative and conductive couplings in a multi-zone structure. Preliminary results from work performed at LBL [2] indicate that the magnitude of the convective heat transfer coefficients on the inside surfaces of a typical direct gain building configuration can vary significantly with time. This result is consistent with an earlier study [3] which demonstrated that appreciable errors in prediction of building thermal loads can result from the common assumption that the total (convective + radiative) heat transfer coefficients are constant with time.

There is evidence that convective heat transfer processes are highly dependent on both the geometric configuration of the structure being studied (e.g. [2]) and the range of thermal boundary conditions that might be encountered in the structure. Also, the natural convection processes which occur in passive systems are largely uninvestigated. Thus, there is a need to provide a sound technical basis for estimating the effects of convection on the performance of buildings. An unmanageably large number of experiments would be required to thoroughly explore natural convection phenomena in buildings empirically. The present study addresses this problem by focusing on the

*This work was supported by the Research and Development Branch, Passive and Hybrid Division, Office of Solar Applications for Buildings, U.S. Department of Energy, under Contract No. 7405-ENG-48.

[+]See Glossary of Technical Terms, Section 8.

development of a general computerized numerical method for analysis of natural convection, and on the validation of the method using results from a few selected experiments. The computer code can then, with some confidence, be applied to a broad range of studies of natural convection in buildings. More specifically, the work reported here consists of:

(1) The development and validation of a numerical analysis technique for studying convective heat transfer in buildings.

(2) The use of this analysis technique to quantitatively study the role of natural convection in the thermal performance of a direct solar gain structure, and thereby to examine the accuracy of standard assumptions regarding convective heat transfer within a zone in a building.

2. BACKGROUND

Past natural convection research [4] has dealt primarily with geometric configurations which do not typify rooms in buildings; as a result, these studies are of limited application in the building sciences. Convective heat transfer coefficients most often used in building energy analysis are largely based on experiments conducted 25 years ago [5,6,7]. This work was necessarily limited in the range of experimental parameters investigated. In addition, the lack of large computers and sophisticated experimental hardware prevented the researchers from thoroughly examining the sensitivity of their results to the experimental assumptions. This past research has not been extended, most likely due to three factors:

(1) The historically low cost of energy used in buildings.

(2) The emphasis on the use of forced convection wherever possible.

(3) The difficulty of conducting analytical, numerical or experimental investigations of configurations representative of buildings.

More recently, there has been renewed interest in natural convection in the building sciences. Investigations of convective heat transfer within and between thermal zones have been reported by Buchberg [3], Nielsen [8], Honma [9], and Weber [10].

3. PROBLEM DEFINITION

In the published literature, the problem of natural convective heat transfer in an enclosure is typically simplified to the configuration illustrated in Fig. 1. In a two-dimensional rectangular enclosure, one vertical surface is maintained at a constant temperature T_H, and the opposite vertical surface is maintained at a lower constant temperature T_C. The horizontal surfaces are adiabatic (perfectly insulated). This was one of the configurations chosen for the numerical and experimental studies for comparisons with published data. Heat input or extraction through one vertical surface of an enclosure is a reasonable model for many situations arising in buildings; for example, it may represent heat gain from an unvented Trombe wall, or heat loss through windows in single and multi-story building. In addition, a previous study [11] indicates that in warm climates the heat losses through the walls and windows (the vertical surfaces) are larger than the losses through the floor and the ceiling (horizontal surfaces) in a well-insulated, single story, residential building.

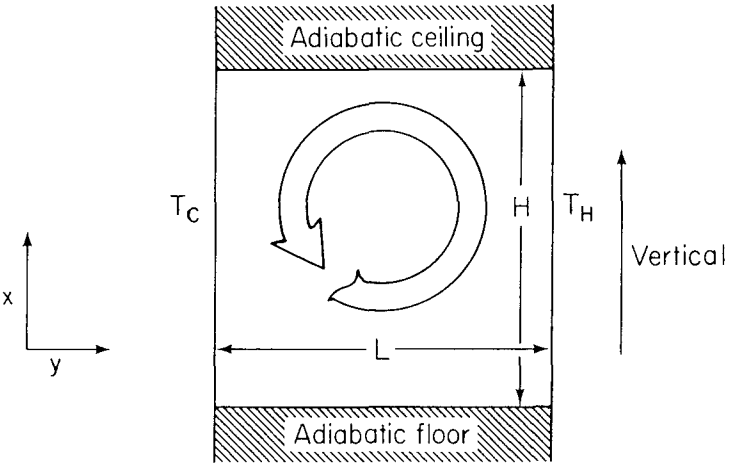

FIGURE 1. RECIRCULATING FLOW INDUCED IN A FLUID INSIDE A TWO-DIMENSIONAL SQUARE CAVITY, DEFINED BY ADIABATIC FLOOR AND CEILING AND ISOTHERMAL WALLS, AT TEMPERATURES T_H AND T_C ($T_H > T_C$).

XBL7911-15125 A

In the configuration illustrated in Fig. 1, variations in density drive the enclosed fluid up the heated wall, along the top horizontal surface, down the cooled wall, and along the bottom horizontal surface, completing the convective loop. The convective motion of the fluid is mostly confined to a thin region along all four internal surfaces, producing a rather large and fairly inactive central core region. Characteristics of the flow such as the mean air temperature, convection coefficients between air and walls, flow velocities, etc., are completely determined by specification of the three independent dimensionless parameters listed below:

(1) Aspect ratio: A = H/L where H = enclosure height and L = enclosure length.

(2) Prandtl number: $Pr = \nu/\alpha$ where ν = kinematic viscosity and α = thermal diffusivity.

(3) Rayleigh Number: $Ra_L = Gr_L Pr = g\beta\Delta TL^3 Pr/\nu^2$, where Gr_L = Grashof number, g = acceleration due to gravity, β = coefficient of thermal expansion, and ΔT = characteristic temperature difference = $T_H - T_C$.

These parameters include all of the relevant information regarding the enclosure geometry, the fluid properties, and the relative strength of buoyancy and viscous forces, respectively. For a rectangular room twice as long (5.5 m) as it is high (2.75 m) filled with air at 21°C and with at least a 1°C temperature difference between vertical walls, these parameters take the values:

$$A = 0.5,$$

$$Pr = 0.71, \text{ and}$$

$$Ra_L \geq 1 \times 10^{10}.$$

4. ANALYSIS DESCRIPTION AND COMPARISON WITH PUBLISHED DATA AT LOW RAYLEIGH NUMBERS

Little numerical work has been published on natural/buoyant convection at Rayleigh numbers in excess of 10^7. In this flow regime fluid velocities become relatively large. If the popular Central Difference Scheme (CDS) is used for casting the equations governing the fluid flow into finite difference form, the large velocities necessitate an impracticably fine mesh size to ensure numerical stability of the solution procedure (e.g. [12]). Spalding [13] has proposed a differencing scheme that overcomes this difficulty; it allows relatively coarse grid spacings without seriously compromising accuracy and solution stability [14]. Two computer programs (CONVEC2 and CONVEC3) were developed based on this differencing scheme. These programs respectively solve the coupled two- and three-dimensional conservation equations with the Boussinesq approximation:

Continuity: $$\text{div}(\vec{V}) = 0$$

Momentum: $$\hat{Re}\,\frac{d\vec{V}}{dt} + (\vec{V}\cdot\vec{\nabla}) = \nabla^2\vec{V} - \text{grad } p + Gr\theta\,\delta_i^3$$

Energy: $$\hat{Re}\,\frac{\partial\theta}{\partial t} + (\vec{V}\cdot\text{grad})\theta = \frac{1}{Pr}\nabla^2\theta.$$

These computer programs can be applied to fluid flow problems driven by predefined temperature distributions on the enclosure surfaces and/or by pressure differentials between specified locations on the boundary. To date, a turbulence model has not been incorporated into either computer program, so the analyses are limited to steady (laminar) flows.* (For a more detailed description of the analysis technique, see [15] and references cited therein.)

Validation of the two computer programs CONVEC2 and CONVEC3 has been undertaken by comparing the calculated results to various published numerical and experimental efforts and by comparison to two recent experiments utilizing room geometries. The comparison to the low Rayleigh number data cited in the literature is described below; validations at the higher Rayleigh numbers characteristic of buildings are described in the next section. It is noted here that the mesh sizes used for calculation in all validations were relatively coarse (the finest two-dimensional mesh size was 17x20). The grid lines were distributed evenly throughout the central region (interior of the fluid volume) with a concentration of grid lines near the enclosure boundaries; this permitted simulation of the sharp changes in flow properties associated with a developed boundary layer. Sensitivity analyses indicated that it was adequate to position three grid lines parallel and adjacent to each enclosure surface for this purpose.

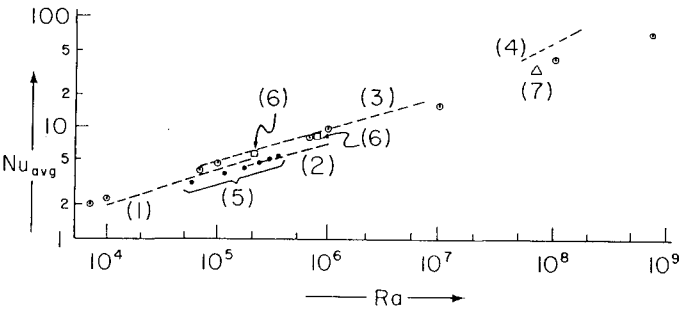

CURVE (1): DE VAL DAVIS CALCULATIONS
CURVE (2): FROM RESULTS OF EMERY, EXPERIMENTAL
CURVE (3): PORTIER ET AL., CALCULATIONS, Pr = 0.7
CURVE (4): BURNAY ET AL., DATA REDUCED FROM EXPERIMENTS, Pr = 0.7
RESULTS (5) ARE OF RUBEL AND LANDIS, CALCULATIONS
RESULTS (6) ARE FROM QUON, CALCULATIONS
RESULT (7) IS FROM FROMM
POINTS INDICATED BY ⊙ ARE FROM PRESENT CALCULATIONS

FIGURE 2. DEPENDENCE OF Nu ON Ra, FOR TWO-DIMENSIONAL FLOW INSIDE A SQUARE CAVITY, COMPARISON WITH PUBLISHED RESULTS.

XBL791I-11123A

*For a room-shaped enclosure, buoyancy-driven convection will not become fully turbulent for Rayleigh numbers less than about 10^{11}. The wind-driven convection in a building is always turbulent.

A quantity of particular importance in the problem defined by Fig. 1 is the magnitude of convective heat transfer, measured by the Nusselt number. For a square enclosure (H = L in Fig. 1), the average Nusselt number can be defined as:

$$\overline{Nu}_L = \frac{1}{T_H - T_C} \int_0^1 \left.\frac{\partial T}{\partial Y}\right|_{Y=0} dX$$

In Fig. 2, Nu_L calculated with the convection code, CONVEC2, is plotted as a function of Rayleigh number. On the same graph, relevant numerical and experimental results for $10^4 \leq Ra_L \leq 10^9$ from various investigators have been superimposed; as shown, the agreement is quantitatively acceptable. Additional validation at low Rayleigh number has been presented in [15].

5. EXPERIMENTS AND ANALYSIS VALIDATION AT HIGH RAYLEIGH NUMBERS

Existing experimental data have largely been limited to Rayleigh numbers of less than 10^9--at least an order of magnitude below that which characterizes full-scale building geometries. In addition, most of these data are for large aspect ratios, typifying fluid flow in narrow vertical channels. Two recent experiments [2,16] have expanded the data base into the geometric and kinematic region of interest to the buildings sciences. The experiments are described below and their results are compared to the predictions of the convection analysis code.

A. Small-Scale Experiment

A small-scale experiment, coordinated with the analysis, is being carried out at Lawrence Berkeley Laboratory. The results from the first phase of this experiment are reported below.

A schematic cross-sectional view of the experimental configuration is shown in Fig. 3; the apparatus has inside dimensions of 12.7 cm height by 25.4 cm length and extends to a horizontal depth of 76.2 cm to minimize three-dimensional effects. Water was used as the working fluid; this allowed representative Rayleigh number values to be obtained in a small-scale apparatus. The range of parameters covered by this experiment are:

$$A = 0.5$$

$$2.6 \leq Pr \leq 6.8$$

$$1.6 \times 10^9 \leq Ra_L < 5.4 \times 10^{10}$$

The opacity of water to thermal radiation implies that the experiment was not a direct, scaled approximation to a real room; however, use of water in the experiment allowed measurement of the purely convective part of

Apparatus Cross-Section

(1) - 1/2" Plexiglas
(2) - 3/16" Copper Sheet
(3) - Water
(4) - Thermofoil heaters
(5) - 3/8" O.D. copper tubing containing cooling water
(6) - High conductivity cement
(7) - 1/4" Plexiglas partition
(8) - Adjustable rod
(9) - 2" Polystyrofoam insulation board
(10) - Inside surface of polystyrofoam lined with polyethylene sheeting
(11) - Airspace
(12) - Thermocouple probe
(13) - Central Thermocouple array
(14) - Fiberglas insulation (2-layers)
(15) - Wood base

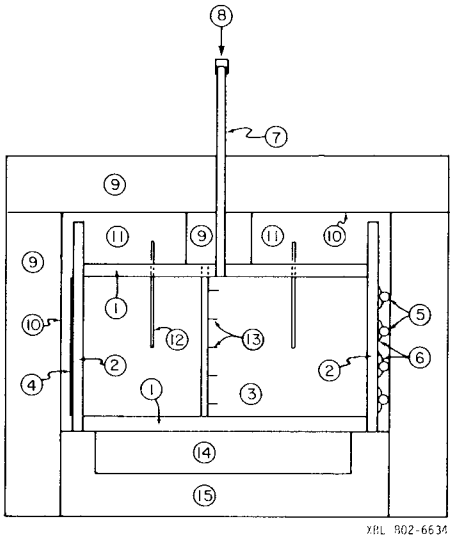

FIGURE 3.

the heat transfer process being studied* and from this standpoint, was ideal for validation of the convection analysis code. It is also noted that in experimental modeling of convective heat transfer processes, the detailed behavior of a fluid with Prandtl number less than 1.0 cannot be accurately simulated with a working fluid having a Prandtl number much greater than 1.0 [17]. Therefore, the magnitude of the Nusselt number measured in this experiment is not numerically identical to that for an air-filled enclosure. However, the general fluid behavior and parametric relationship observed in the experiment can be expected to be representative of an air-filled cavity.

The heat transfer data obtained from the experiment are presented in the form of $Log_{10}(Nu_{L_{IN}})$ vs. $Log_{10}(Ra_L)$ in Fig. 4. In this figure, $Nu_{L_{IN}}$ (Nusselt number) is a measure of the strength of the convective heat transfer at the heated wall. On the same figure, experimental results from a study by MacGregor and Emery [17], and predictions from an analytic study by Raithby et al. [18] are shown; the present experiment

*The maximum contribution of thermal radiation to the measured Nusselt number was calculated to be less than 2%.

FIGURE 4. Heat transfer results and comparison

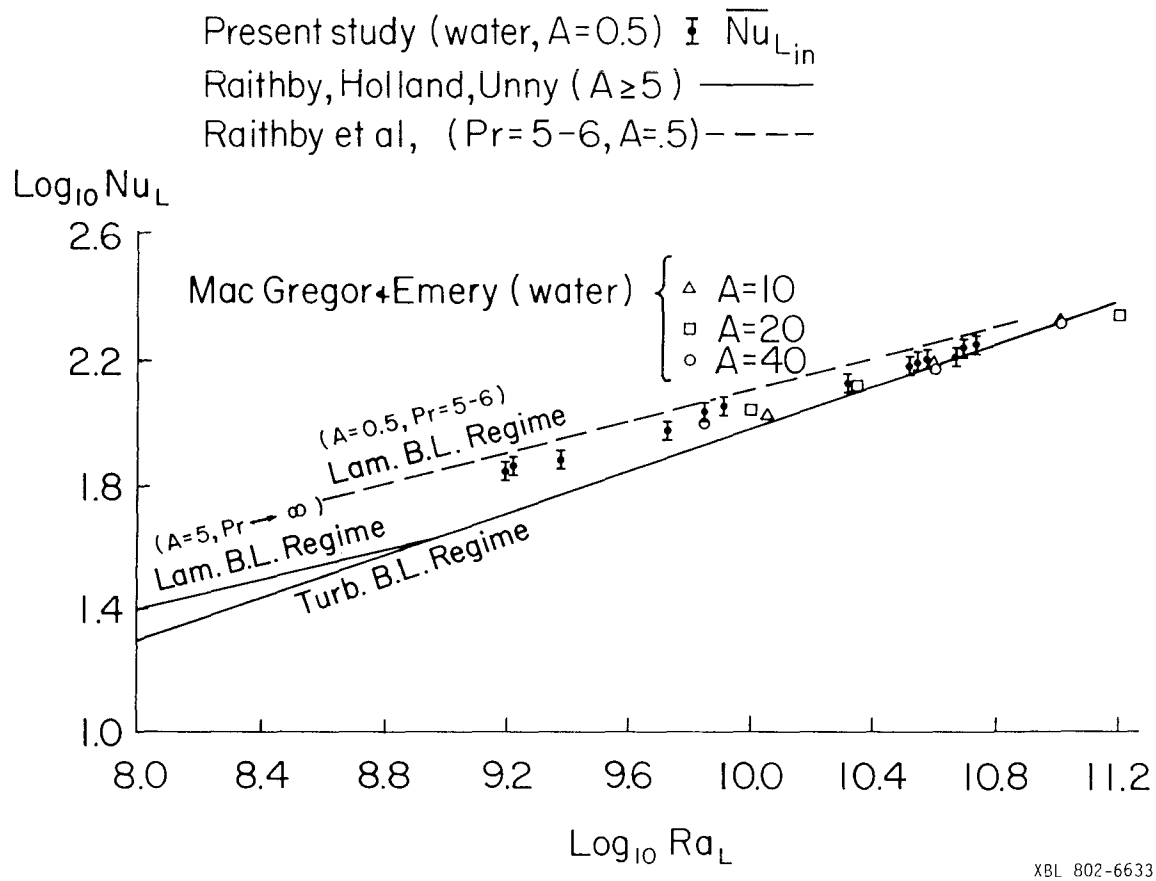

XBL 802-6633

is in quantitatively good agreement with both of these previous results. (At the high Rayleigh numbers shown in the figure, the Nusselt number is relatively insensitive to the aspect ratio [19,20].)

In order to use the data from this experiment for validation of the two-dimensional convection code, the computer program was modified to incorporate the temperature dependence of the physical properties of water. Sensitivity studies using the computer program demonstrated an increase of up to 10% in the Nusselt numbers when the properties were allowed to vary with temperature rather than being fixed at their average values. Due to lack of sufficiently detailed experimental instrumentation, best estimates of some enclosure surface temperature profiles were necessary to complete the input to the analysis program. These surface temperature estimates are believed to have errors of less than ±10%. To date, the sensitivity of the prediction of the computer code to these uncertainties has not been thoroughly investigated, pending the availability of data from an improved small scale experiment in progress at LBL.

Comparisons of the predictions of the computer code with the experimental results for the extent of stratification in the core region are shown in Figs. 5 and 6. These figures show the temperature profiles along vertical and horizontal lines through the geometric center of the enclosure for Ra_L = 2.4×10^9 and $Ra_L = 4.7 \times 10^{10}$, respectively. The excellent agreement of the numerical prediction of the temperature profiles in the central core at the lower Rayleigh number (Fig. 5) indicates that the program is addressing the fundamental characteristics of the flow succesfully at this Rayleigh number (2.4×10^9). The numerically predicted vertical centerline temperature profile at the higher Rayleigh number (4.7×10^{10}, Fig. 6) exhibits a shift to smaller temperature gradients in the central core region associated with an increased gradient near the horizontal surfaces. The most likely source(s) of this discrepancy are: (1) The potential for transitional flow (between steady laminar and fully turbulent) at this value of Ra_L could contribute to the noted differences between experiments and numerical results; (2) due to increased convective effects at this higher Ra_L the errors in the estimates of surface temperatures immediately upstream from the centerline region may have a significant effect on the magnitude of the calculated temperature profile at the centerline; (3) the coarse mesh size used in the present numerical studies may have been a contributing factor to the disagreement at this high value of Ra_L. Ongoing work is presently expected to shed some light on this question; until the source of the discrepancy is under-

stood, however, the comparison of stratification profiles implies that the convection code properly represents the fundamental character of the flow for the smaller value of Ra_L and is qualitatively correct for all $Ra_L < 5 \times 10^{10}$.

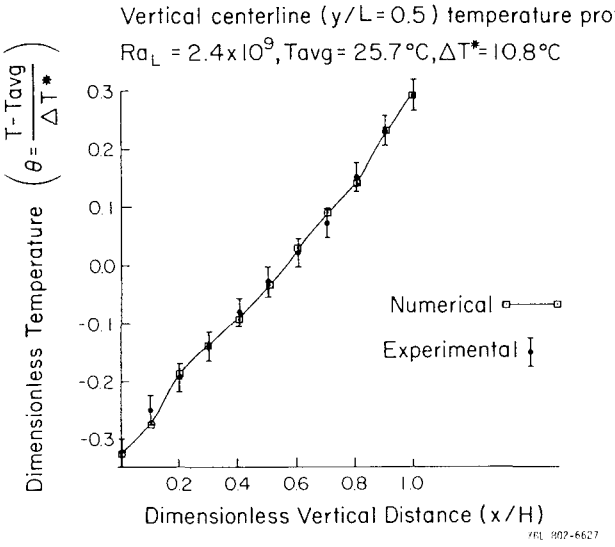

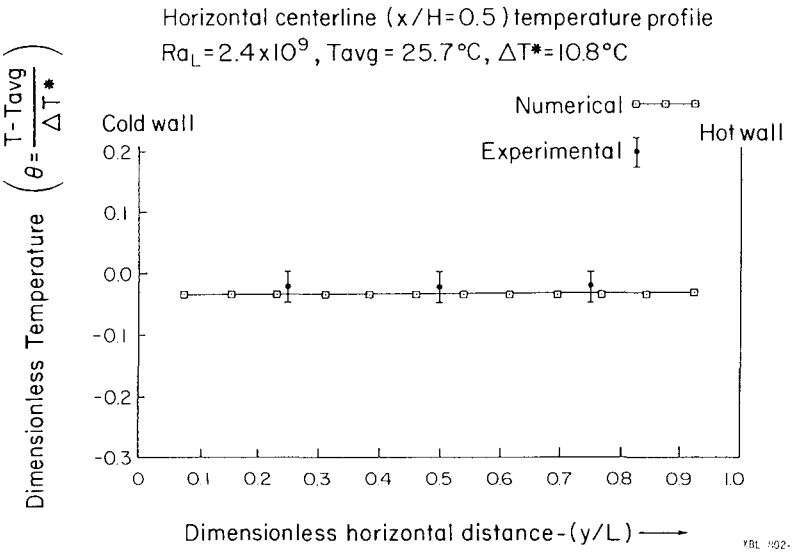

FIGURE 5.

The Nusselt number predictions made by the computer code are compared to the corresponding measurements in Table 1; the surface temperature distributions used in the simulations are also indicated in this table. The two separate numerical simulations (Runs 2a and 2b) made at the higher Rayleigh number give an indication of the sensitivity of the predicted Nusselt number to differences in the details of a surface temperature specification. The disagreement in the Nusselt numbers at the lower Ra_L is thought to be due to this noted sensitivity of the Nusselt number prediction to the details of the (unmeasured) surface temperature distributions.

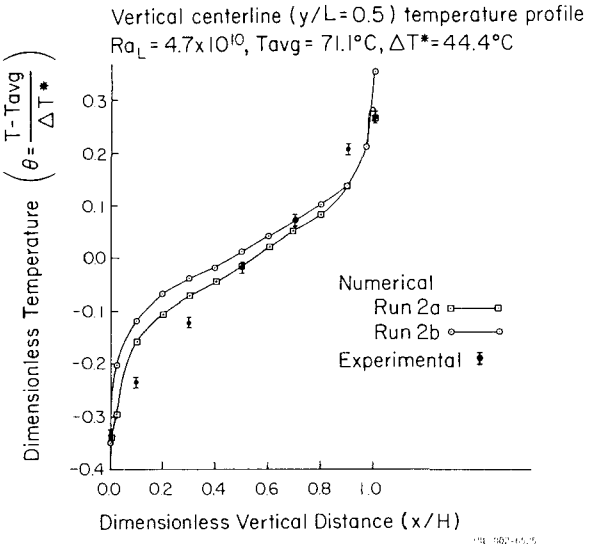

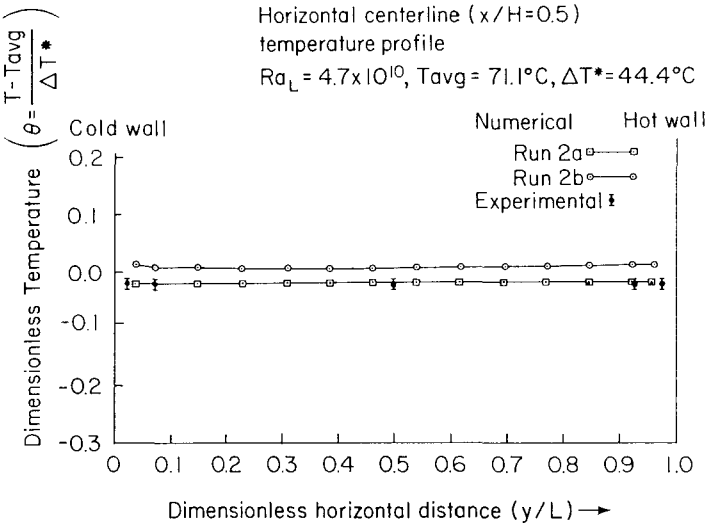

FIGURE 6.

TABLE 1. COMPARISON OF HOT WALL $\overline{Nu}_{L_{IN}}$

RUN	Ra_L	EXPT'L	NUMERICAL	SURFACE TEMPS FOR NUMERICAL SIMULATIONS
1	2.4×10^9	79 ± 12	105	ESTIMATED FROM EXP'T
2a	4.7×10^{10}	165 ± 12	168	ESTIMATED FROM EXP'T
2b			201	HOT & TOP WALL = T_H, COLD & BOTTOM WALL = T_C

B. Full-Scale Experiment

Natural convection was investigated by Ruberg [16] at the Massachusetts Institute of Technology in a full-sized test room shown schematically in Fig. 7. The conditions of this experiment are not as simplified as described in Section 3 and correspond more closely to those in a real building. Heat

was supplied to the test room by an electric resistance heater plate on the floor. A single-pane window was located on one wall of the enclosure. Though the window represents only 2% of the envelope area of the test room, it dominated the thermal load; 22% of the total heat loss was measured to be through this surface. Steady-state conditions were maintained by controlling the temperature of the air outside the test room to within $\pm 0.2^{o}C$ of its average value. The construction was sufficiently airtight that the effects of infiltration could be ignored.

Schematic diagram of Ruberg's full-scale test.

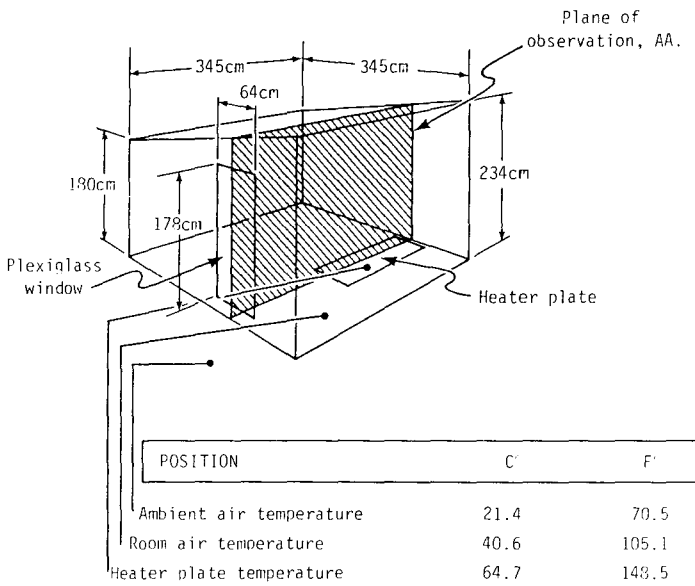

POSITION	C°	F°
Ambient air temperature	21.4	70.5
Room air temperature	40.6	105.1
Heater plate temperature	64.7	148.5

XBL7911-13133A

FIGURE 7.

The heater plate configuration was intended to represent a solar irradiated area on the floor; its rectangular shape and its size (1.16 m^2) were well-matched to those of the 1.12 m^2 window, and its heating capacity (448 W/m^2) was selected to approximate solar radiation falling on a dark-colored floor with low thermal capacity at noon on a clear day at $40^{o}N$ latitude. The parameters for this experiment were:

$$A = 0.58$$

$$Pr = 0.71$$

$$Ra_L = 5 \times 10^{10}$$

Convection observed in the test room was characteristic of the transition regime, between laminar and turbulent flow. A schematic of the air flow patterns is shown in Fig. 8. Note the essentially three-dimensional character of the flow.

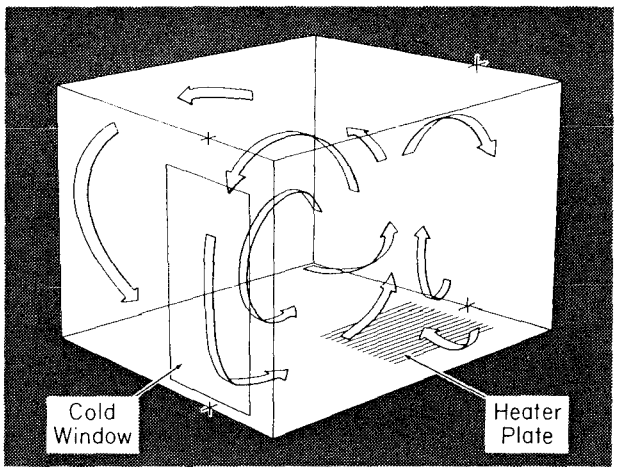

SCHEMATIC OF AIR-FLOW PATTERNS IN RUBERG'S EXPERIMENT

XBL 807-7176

FIGURE 8.

Air temperatures were measured with a vertical array of eleven thermistors mounted on a motorized boom which traversed the test room in the measurement plane. The array had 20 cm vertical spacings in the center and 10 cm spacings near the ceiling and floor; data were recorded at 20 cm horizontal intervals as the boom moved across the room. This resulted in a grid of 11x18 temperature data points in the measurement plane which perpendicularly bisects the window and the heater surfaces (plane AA in Fig. 7).

Temperature measurements were converted to isotherms separated by intervals of 5% of the maximum surface-temperature difference in the room. The isotherms were referenced to the mean temperature of the room, indicated on Fig. 9 as 0.00. The three sets of isotherms represent data from three separate measurements of air temperatures under identical conditions. From the isotherms, the air flow patterns shown in Fig. 8 may be discerned: the plume over the heater plate, a layer of warm air at the ceiling, a cool air current at the window and along the floor, and a somewhat isothermal area in the center of the room. For more details of this experiment, see Ref. [16].

Data from this full-scale experiment were compared with the predictions from the three-dimensional version of the numerical code. The surface temperature profiles used in the analysis were estimated from the available data using a thermal balance technique. It is noted that the effects of radiation on the temperature probes are expected to bias the measured air temperatures towards higher values by an unknown amount. This effect was not accounted for in the thermal balance. This bias also affects the comparisons between the isotherms predicted by the numerical scheme (Fig. 10) and the experimental results (Fig. 9). Also, as noted above,

the observed flow was in the transition regime (between laminar and fully turbulent), but was simulated with a numerical code assuming laminar flow. In light of these limitations the agreement is considered satisfactory.

The above reported validations have been performed with the available experimental data covering the range of interest of the important dimensionless parameters. The discrepancies between the predictions and the observations are thought to be understood, at least qualitatively. The computer program appears to simulate the convective flow correctly for $Ra_L < 5 \times 10^{10}$. The second phase of the ongoing small-scale experiment at LBL is expected to provide a quantitatively sound basis for further validation of the computer code at higher Rayleigh numbers.

The computer program, validated to the extent possible with the available data, has been used to study the influence of natural convection on the thermal performance of a single room in a direct gain passive solar building; this is described in the next section.

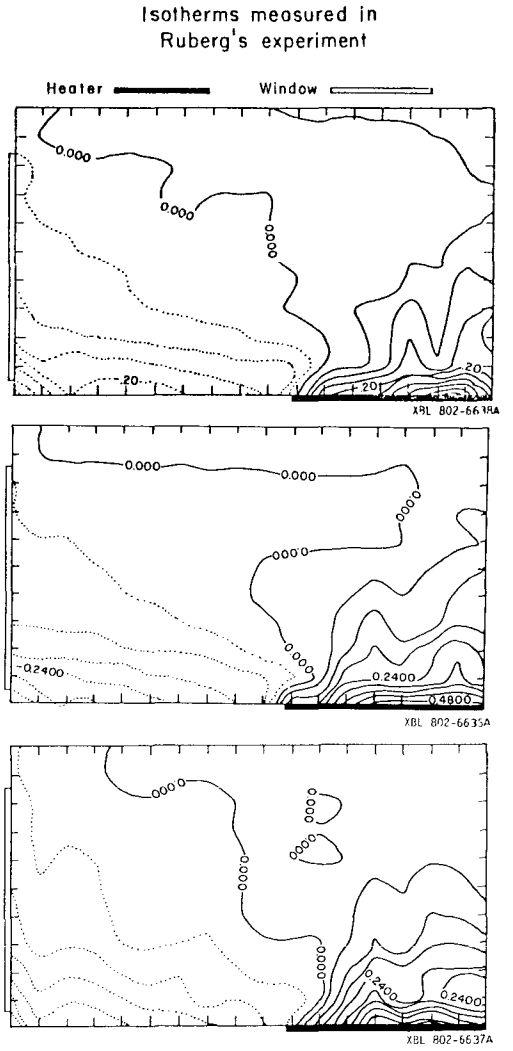

FIGURE 9.

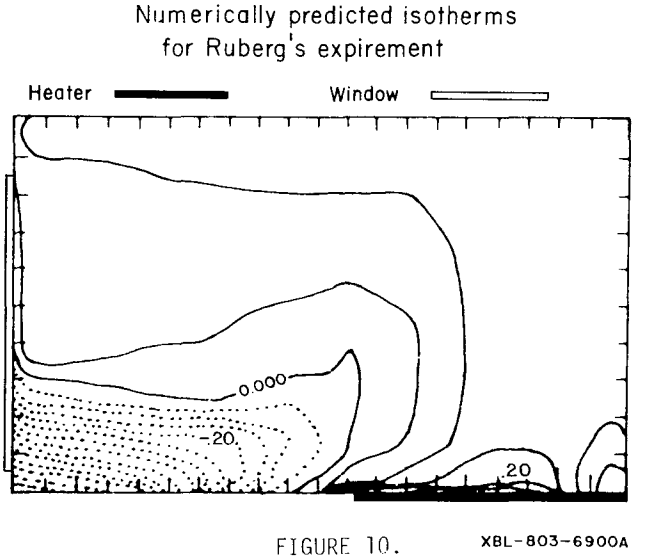

FIGURE 10. XBL-803-6900A

6. CONVECTION EFFECTS IN BUILDING ENERGY ANALYSIS

Most building energy analysis techniques, including the most sophisticated computer codes (BLAST,* DOE-2,† etc.) and other passive solar system analysis programs, make the simplifying assumptions that (1) the air temperatures throughout the volume of the individual zones in the structure are uniform, and (2) the convective heat transfer coefficients for the surfaces of the building being analyzed are constants. These assumptions are largely consistent with the state of knowledge regarding convection at the time the codes were developed.§ In a preliminary study [15], it was shown that convection coefficients at the surfaces of an enclosure are actually quite sensitive to the temperature distributions on the surfaces. In order to estimate the effects of this observation on the accuracy of results from the programs, the convection code was used iteratively with BLAST to obtain self-consistent surface temperature distributions

*BLAST (Building Loads Analysis and System Thermodynamics) is copyrighted by the Construction Engineering Research Laboratory, U.S. Dept. of the Army, Champaign, Illinois.

†DOE-2 is a public domain program being developed by the Division of Communities and Building Energy Systems, Department of Energy.

§ Some of the codes do utilize convection coefficients for non-vertical surfaces which are sensitive to the direction of heat flow, but not to the magnitude of the temperature difference between the room air and surface or to the possibly large effects induced by the differences in the temperatures of the different surfaces defining the zone.

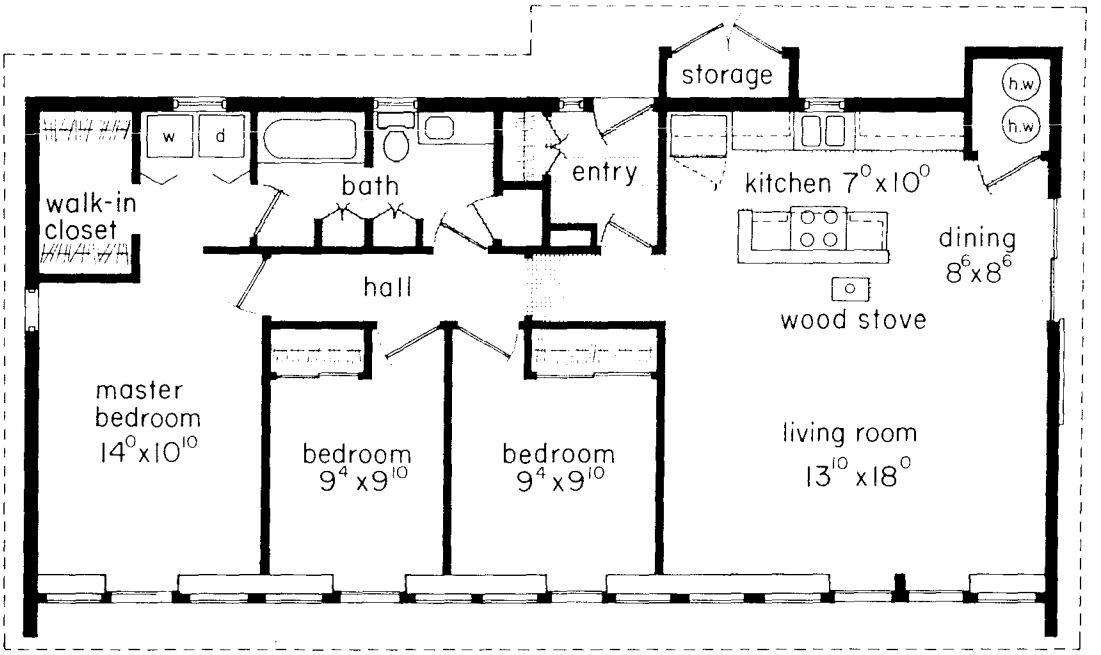

FIGURE 11a. Floor plan of TVA house.

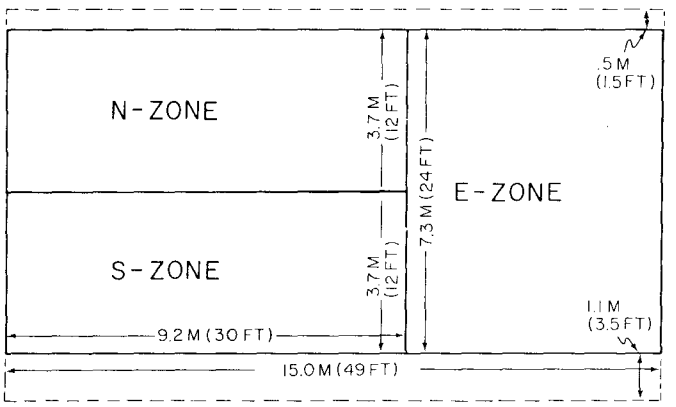

Floor plan showing thermal zones for blast simulation.

FIGURE 11b.

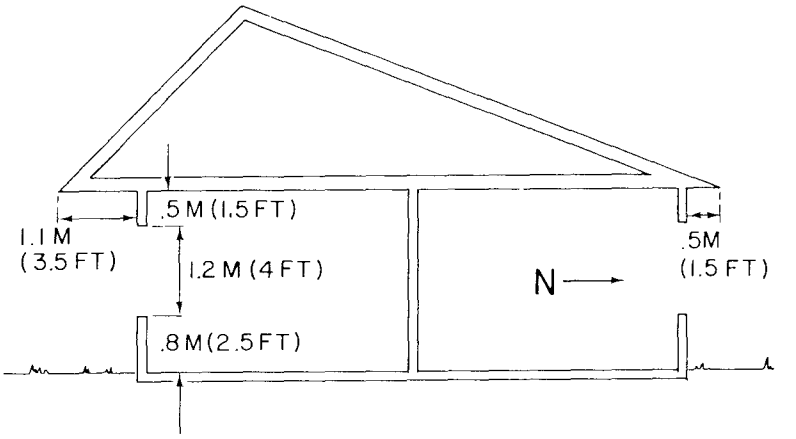

FIGURE 11c. Cross section for blast simulation.

Convection Coefficients (Watts/m^2-°C) between the room air and the interior sub-surfaces of a single zone in a house. Steady State (Day time) heat gain mode.

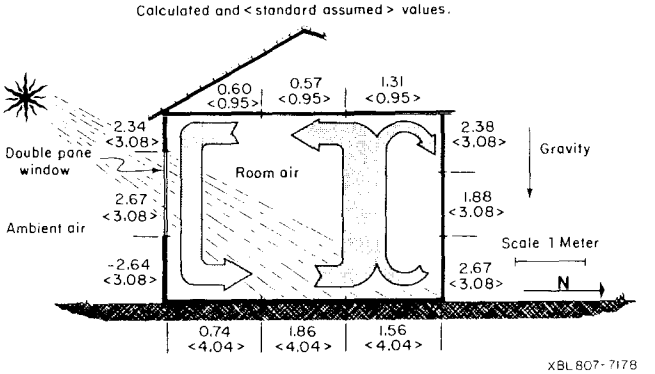

FIGURE 12.

and convection coefficients.*

The south facing zone (S-zone in Fig. 11b) of a multi-zone building was studied. The floor plan of the building is shown in Fig. 11a. Figures 11b and 11c show the thermal zones used in the BLAST simulations. The building has been thoroughly described elsewhere [28]. This zone has dimensions of 3.66 m wide x 9.14 m long x 2.44 m high. For the purpose of this study, the following modifications to the zone were made. The interior of the analyzed zone was made up of 14 surface segments. The two "end surfaces" (the east partition wall and the west exterior wall) measured 2.44 m x 3.66 m and were very highly insulated. The other four major surfaces (ceiling, slab floor, gypboard north partition wall, and the south exterior wall) were each divided into three equal subsurfaces (see Fig. 12). The individual subsurface extended the full 9.14 m length of the zone. The middle section of the south wall was specified as double-pane window. Iterative analyses were performed for both the nighttime (loss) and daytime (gain) mode for a selected winter design day; this procedure is described below.

For each iterative sequence of calculations, BLAST was first used to calculate the surface temperatures of each subsurface defining the zone for each hour of the design day using the standard constant convection coefficients. BLAST performs a full thermal balance on all surfaces of the zone under study and the zone air. The surface thermal balance accounts for: thermal radiation between zone surfaces; convection between zone air and each surface; conduction through each surface; and radiative gains from occupants, lights, equipment, and transmitted solar energy. The thermal balance on the air accounts for convective gains from surfaces, occupants, lights and equipment, and for controlled and uncontrolled ventilation. For this study, the relevant output from BLAST was the distribution of temperatures of the subsurfaces defining the zone boundary. From the design day results, two hours were chosen for further analysis of convection: one hour at night when the zone is in the loss mode and one hour during midday when the zone is in the solar gain mode.

Due to the zone geometry and the distribution of the surface temperatures, the convective flow was expected to be two-dimensional in character. The individual subsurface temperatures calculated by BLAST were input to the two-dimensional convection code in order to simulate the details of the convection process and calculate convective heat transfer coefficients for each subsur-

*The convective heat transfer coefficient (CHTC) for a given surface is defined by the relation CHTC = $q/\Delta T$ where q = heat flux from the surface into the room air, ΔT = (average surface temperature) - room air temperature).

Surface Temperatures (°C) on the interior sub-surfaces of a single zone in a house. Steady State (Day time) heat gain mode.

With calculated and < with standard assumed > convection coefficients.

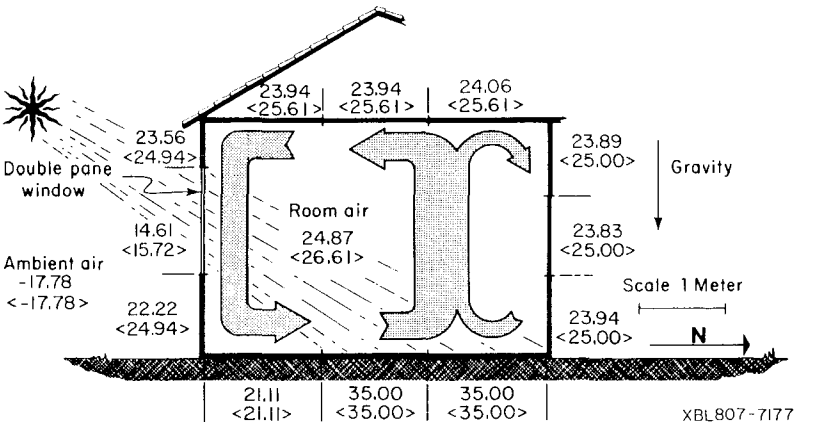

FIGURE 13.

Convection Coefficients (Watts/m^2-°C) between the room air and the interior sub-surfaces of a single zone in a house. Steady State (Night time) heat loss mode.

Calculated and < standard assumed > values.

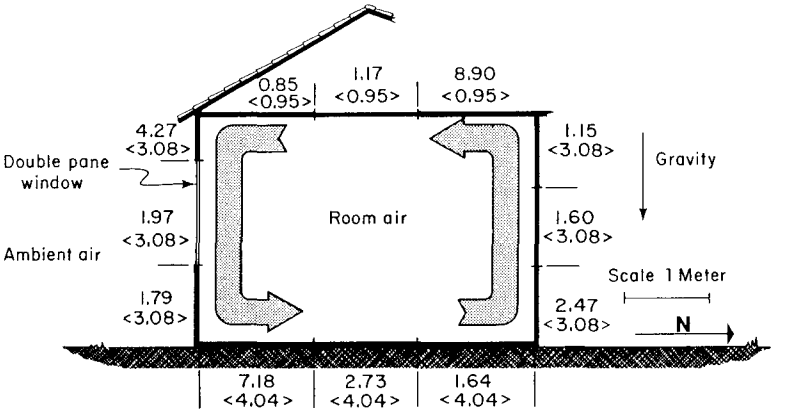

FIGURE 14.

Surface Temperatures (°C) on the interior sub-surfaces of a single zone in a house. Steady State (Night time) heat loss mode.

With calculated and < with standard assumed > convection coefficients.

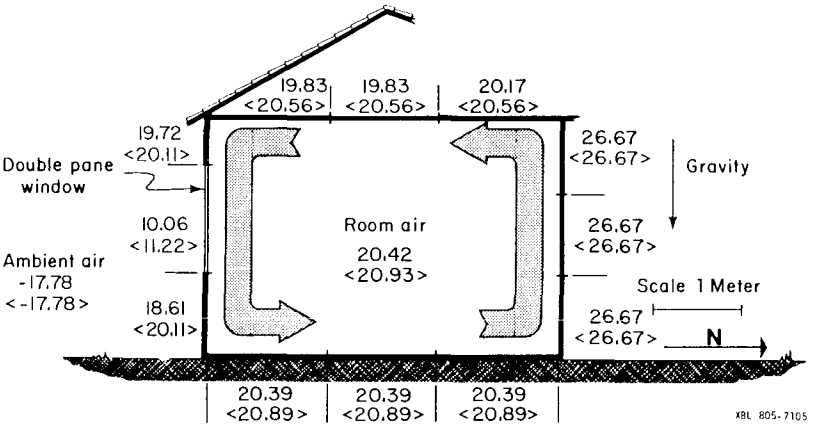

FIGURE 15.

face. These coefficients were then used as input to BLAST to obtain the new subsurface temperatures. These temperatures were again used as input to the convection code and the entire procedure was iterated until self-consistent results were obtained. Several features of the iteration process should be noted here:

(1) The convection code, at its present state of development, cannot account for sources and/or sinks of thermal energy in the air volume under study. For this reason, the BLAST simulation did not include auxiliary heating and/or cooling of the zone in which the convection was to be analyzed; the zone temperature was free-floating, although adjacent zones were heated. This limitation led to the selection of an exterior dry bulb temperature for the design day such that the zone air temperature would float near a typical daytime thermostat (nighttime thermostat setback) temperature. These temperatures are shown in Figs. 13 and 15.

(2) During the loss mode (nighttime) iterations, the north partition wall, representing a warm storage wall, and properly accounting for the existence of a conditioned zone to the north, was held at a constant temperature and was the primary heat source for the zone. During the gain mode (daytime), only the two subsurfaces of the slab floor closest to the north partition wall were irradiated by solar transmission through the south glazing. This configuration corresponds to midday conditions during the winter (solar altitude = 30^{o}). These subsurfaces were the primary heat source for the zone and their surface temperatures were held constant throughout the iteration process. Here too, the effect of the adjacent conditioned zones was properly accounted for by the BLAST analysis. The glass was also held at a constant surface temperature during the gain mode.

(3) A design day with varying ambient temperatures and other environmental parameters was initially used to calculate the starting points for the iteration scheme; however, during the iterations, steady-state external conditions were assumed in order to observe convergence more clearly. As noted in (1) above, since the BLAST simulations assumed no auxiliary heating or cooling in the zone being analyzed, the exterior temperature was selected to ensure that reasonable comfort conditions were maintained in the zone with the specified constant surface temperatures described in (2) above.

The results of the detailed convection analysis are summarized in Figs. 12-15. The surface temperatures and convective coefficients obtained both with and without the iterative procedure using the convection code are shown in these figures. More detailed heat transfer data for the two modes is given in Tables 2 and 3. In these tables, subsurfaces are numbered sequentially around the zone; results for the thermal parameters for each subsurface appear in the table. Case I refers to standard assumptions and Case II refers to the converged values resulting from the iterations.

The convection coefficients are seen to change substantially from their standard assumed values for most of the surfaces. This is particularly true during the loss

TABLE 2. CONVECTIVE ANALYSIS OF A SINGLE ZONE, GAIN MODE

SURFACE	SUBSURFACE NUMBER	SUBSURFACE LOCATION	STANDARD BUILDING ENERGY ANALYSIS ASSUMPTIONS				VALUES AFTER ITERATION WITH CONVECTION CODE			
			SURFACE TEMP ^{o}C	CONVECTION COEFFICIENT $W/m^2/^{o}C$	CONVECTIVE HEAT FLUX FROM ZONE TO SURFACE W/m^2	TOTAL HEAT FLUX FROM ZONE TO SURFACE W/m^2	SURFACE TEMP ^{o}C	CONVECTION COEFFICIENT $W/m^2/^{o}C$	CONVECTIVE HEAT FLUX FROM ZONE TO SURFACE W/m^2	TOTAL HEAT FLUX FROM ZONE TO SURFACE W/m^2
SOUTH	1	TOP	24.94	3.08	5.14	20.34	23.56	2.34	3.63	19.78
EXTERIOR	2	MIDDLE/WINDOW	15.72	3.08	33.54	163.85	14.61	2.67	27.10	151.98
WALL	3	BOTTOM	24.94	3.08	5.14	20.34	22.22	-2.64	-7.81	19.21
SLAB-ON-	4	SOUTH	21.11	4.04	22.22	60.46	21.11	0.74	2.98	44.64
GRADE	5	MIDDLE	35.00	4.04	-33.89	-159.89	35.00	1.86	-18.30	-142.94
FLOOR	6	NORTH	35.00	4.04	-33.89	-159.89	35.00	1.56	-15.40	-137.30
NORTH	7	BOTTOM	25.0	3.08	4.96	19.21	23.94	2.67	3.08	15.26
PARTITION	8	MIDDLE	25.0	3.08	4.96	19.21	23.83	1.88	2.54	15.26
WALL	9	TOP	25.0	3.08	4.96	19.21	23.89	2.38	2.98	15.26
CEILING	10	NORTH	25.61	0.95	0.95	11.86	24.06	1.31	1.45	11.86
TO	11	MIDDLE	25.61	0.95	0.95	11.86	23.94	0.57	0.65	11.86
ATTIC	12	SOUTH	25.61	0.95	0.95	11.86	23.94	0.60	0.69	11.86
			T_{AIR} = 26.61, T_{MRT} = 25.91				T_{AIR} = 24.87, T_{MRT} = 24.83			

T_{AIR} = Average Temperature of Air in the Zone

T_{MRT} = Mean Radient Temperature in the Zone.

TABLE 3. CONVECTIVE ANALYSIS OF A SINGLE ZONE, LOSS MODE

SURFACE	SUBSURFACE NUMBER	SUBSURFACE LOCATION	STANDARD BUILDING ENERGY ANALYSIS ASSUMPTIONS				VALUES AFTER ITERATION WITH CONVECTION CODE			
			SURFACE TEMP °C	CONVECTION COEFFICIENT $W/m^2/°C$	CONVECTIVE HEAT FLUX FROM ZONE TO SURFACE W/m^2	TOTAL HEAT FLUX FROM ZONE TO SURFACE W/m^2	SURFACE TEMP °C	CONVECTION COEFFICIENT $W/m^2/°C$	CONVECTIVE HEAT FLUX FROM ZONE TO SURFACE W/m^2	TOTAL HEAT FLUX FROM ZONE TO SURFACE W/m^2
SOUTH EXTERIOR WALL	1	TOP	20.11	3.08	2.53	7.46	19.72	4.27	2.99	6.91
	2	MIDDLE/WINDOW	11.22	3.08	29.91	83.87	10.06	1.97	20.41	77.18
	3	BOTTOM	20.11	3.08	2.53	7.46	18.61	-1.79	-3.24	7.03
SLAB-ON-GRADE FLOOR	4	SOUTH	20.89	4.04	0.16	0.57	20.39	7.18	0.22	0.28
	5	MIDDLE	20.89	4.04	0.16	0.57	20.39	2.73	0.08	0.14
	6	NORTH	20.89	4.04	0.16	0.57	20.39	1.64	0.05	0.11
NORTH PARTITION WALL	7	BOTTOM	26.67	3.08	-17.68	-51.91	26.67	2.47	-15.44	-52.91
	8	MIDDLE	26.67	3.08	-17.68	-51.91	26.67	1.60	-10.02	-47.49
	9	TOP	26.67	3.08	-17.68	-51.91	26.67	1.15	-7.20	-44.67
CEILING TO ATTIC	10	NORTH	20.56	0.95	0.35	2.67	20.17	8.90	2.22	3.55
	11	MIDDLE	20.56	0.95	0.35	2.67	19.83	1.17	0.69	3.98
	12	SOUTH	20.56	0.95	0.35	2.67	19.83	0.85	0.50	3.79
			T_{AIR} = 20.93, T_{MRT} = 20.96				T_{AIR} = 20.42, T_{MRT} = 20.40			

T_{AIR} = Average Temperature of Air in the Zone, °C

T_{MRT} = Mean Radient Temperature in the Zone, °C

mode in which strong boundary-layer flows develop along both the warm North wall and the cold South window. During the gain mode, circulation induced by large, warm areas of the floor does not contain such strong boundary layer flows. The balance point air temperature (mean radiant temperature) for the zone is observed to change by 0.51°C (0.56°C) and 1.74°C (1.08°C) for the loss and gain modes, respectively.

The thermal behavior of the zone during the loss mode changes less than might be expected. The following considerations are relevant to this observation:

(1) The surfaces which are coupled to the room air through larger convection coefficients in Case II have smaller resulting temperature deviations from the room air temperature than in Case I. On the other hand, the surfaces which are coupled to the room air through smaller convection coefficients in Case II tend to have larger resulting temperature deviations from the room air than in Case I. This has a moderating influence on what otherwise would have been larger changes in the convective (and radiative) heat fluxes.

(2) Radiative exchange is of the same order of magnitude as convection in thermally coupling the zone surfaces to one another. For this reason, changes in the convective heat flux will have a smaller percentage effect on the total heat flux (convection + radiation) from a surface.

During the loss mode, the convective heat flux from the warm north wall shows a significant variation along its height (15.4 W/m^2 from the bottom of the wall to 7.2 W/m^2 from the top). As cold air warms up at the bottom of the north wall and rises, the upper portions of the wall encounter relatively warmer air and can contribute relatively less heat to this air. If this north wall were a heat storage system, the convective recovery of heat from the bottom portions of the wall would be nearly twice as rapid as that from the top portions, in this configuration. Another interesting feature is the very large convective coefficient (8.9 $W/m^2°C$) for the portion of the cool ceiling directly warmed by the updraft from the warm north wall. Since the ceiling was well insulated, the temperature difference between this portion of the ceiling and the room air was decreased (by about 50%) with only a neglible change in the heat loss to the attic.

During the gain mode, the results presented in Table 3 show that the convective heat transfer from the floor to the air is reduced by about a factor of two when correct convection coefficients are used. This contributes to the observed lowering of the air temperature in the zone. Total heat transfer to the non-illuminated massive north partition wall is reduced by only approximately 20%. Also, losses from the south window are reduced by about 8%; this change is about equally split between reductions in convection and radiation.

During both modes of operation, the portion of the south wall directly below the double-pane window encounters a downdraft of cold air that has lost heat through the window. This downdraft of air is actually colder than the interior surface of the bottom portion of the south wall (this surface is warmed by radiative exchange with the other surfaces of the zone). Thus, although the bottom section of the south wall is actually

cooler than the average room temperature, it deposits heat into the cold downdraft flowing across it. This has resulted in a negative convective coefficient for this subsurface (the convective coefficients are defined with respect to the average room air temperature).

From a practical viewpoint, convection coefficients and surface temperatures are of little real interest except as they influence comfort levels and/or thermal load. Here, the building load is a quantity of fundamental interest. To estimate the effect on the thermal load of change in any building parameter, the accepted "exact" method i.e., co-heating, is described as follows: The building temperature is maintained at a constant level before and after the parametric change by introducing a heat source/sink of appropriate magnitude. The difference between the heat supplied/removed by the source/sink in the two cases gives the effect of the parametric change on the building load [29].

Since the BLAST simulations described here did not include heat sources/sinks, a less exact method based on the balance point air temperature was necessarily used to estimate the effect of the changed convection coefficients on the zone load. This method was calculated (using a radiation balance technique) to be in error by less than 2% (with respect to the results of the "exact" coheating method) for the configuration under study.

The zone under examination was simulated by BLAST with two different thermostat control profiles. The "base case" thermostat settings were (arbitrarily) set at 21.1°C (70.0°F) for daytime (gain mode) heating and 16.7°C (62.°F) for nighttime (loss mode) heating. The base simulation assumed the same external weather conditions as used in the iteration procedures for the two modes of operation. Iterations with the convection code had predicted changes in the balance point air temperatures of 1.7°C and 0.5°C for the gain and loss modes respectively. The net effect of the balance point change would be to decrease the cooling load and/or increase the heating load. Therefore, during the second load calculation the second thermostat profile was set at 22.8°C (21.1°C + 1.7°C) for daytime heating and 17.2°C (16.7°C + 0.5°C) for nighttime heating.

The results of the BLAST runs using these two different thermostat control profiles are shown in Table 4. The calculated percentage increase in the zone load for this particular case is seen to be quite large. It is noted that the small magnitude of the calculated thermal load represents the load through one external wall of one zone, and is only a fraction (about 20%) of the total building load.

TABLE 4.

INFLUENCE OF VARIABLE CONVECTION COEFFICIENTS ON CALCULATED THERMAL LOADS FROM BLAST

THERMOSTAT SETTINGS		CORRESPONDING CONVECTION COEFFICIENT ASSUMPTION	CALCULATED THERMAL LOAD* KWH/DAY
T_{DAY} (7:00 AM TO 11:00 PM) °C	T_{NIGHT} (11:00 PM TO 7:00 AM) °F		
21.1	16.7	CONSTANT	1.97
22.8	17.6	VARIABLE	2.93

*ASSUMING NO INTERNAL LOADS AND NO INFILTRATION

The results presented here suggest that energy analysis of passive solar systems must include a more detailed representation of natural convection processes than current techniques allow. The iterative procedure described in this section has intentionally assumed somewhat oversimplified building occupancy, and performance parameters (e.g., no internal loads, no infiltration, etc.). Though the example is not directly representative of real buildings, the simplifying assumptions are not expected to be the source of the observed discrepancies. These discrepancies are not expected to have been amplified by the simplifying assumptions unless the building is so dominated by occupant effects and operation that the natural convection processes become relatively small in comparison to forced convection. This is contrary to experience (e.g., [1]) and to intuition. In order to more definitively assess the importance of convection effects on building loads, the convection analysis code described here will be modified. The new program will allow the addition of heat sources/sinks to the enclosure so that the balance point approach to calculating the change in building load can be replaced with the more exact coheating analysis. In addition, the capability of modeling turbulence is also planned.

7. SUMMARY

A numerical technique for modeling natural convection in room geometries has been developed. The numerical predictions from this technique have been compared with various published data and demonstrate satisfactory agreement. The results from a small-scale and a full-scale experiment studying natural convection in room geometries have been presented. The numerical predictions are compared with the results of these experiments; the agreement is also satisfactory. The convection code has been used in conjunction with the BLAST computer program to investigate the thermal behavior of a realistic direct-gain zone configuration. The results indicate that:

- The detailed modeling of convection may have a significant effect on the zone air temperature and the mean radiant temperature.
- More carefully calculated values of the convective coefficients can be substantially different from the values that are currently assumed by the standard building energy analysis methods.
- The convection coefficients for a particular surface can have large diurnal variations.
- The convective coefficients can show a significant variation across a given zone surface.
- Such variations in convective coefficients may have substantial effects on thermal loads for a structure.

8. GLOSSARY OF TECHNICAL TERMS

Buoyancy Driven Convection: Convection driven by differences in the density of air at different temperatures within a space. This is sometimes also referred to as free or natural convection.

Zone: A room (or enclosure) in a building within which the air temperature (or comfort conditions) can be assumed to be homogeneous to an adequate approximation. These comfort conditions can then be calculated from the incident solar radiation, heat gain/losses through the exterior surfaces of the zone, internal heat gain within the zone, the rate of air exchanged with the outdoor environment and neighboring zones, etc.).

9. NOMENCLATURE

A	Aspect ratio = H/L
C_p	Specific heat at constant pressure
Gr_L	Grashof number = $g \cdot \beta \cdot \Delta T \cdot L^3/\nu^2$
g	Acceleration due to gravity
H	Enclosure height
L	Enclosure length
$\overline{Nu}_L$	Average Nusselt number = $gL/\Delta T\kappa$
$\overline{Nu}_{L_{IN}}$	Average Nusselt number on the hot wall
p	Dimensionless pressure
Pr	Prandtl number = ν/α
q	Heat flux
Ra_L	Rayleigh number = $Gr_L \cdot Pr$
$\hat{Re}$	Dimensionless scale of time
T	Temperature
ΔT	Characteristic temperature difference, = $T_H - T_C$
ΔT^*	Maximum temperature on hot wall - Minimum temperature on cold wall
t	Dimensionless time
T_{AIR}	Average temperature of air in the zone
T_{MRT}	Mean radiant temperature in the zone
T_C	Average temperature of the cold wall
T_H	Average temperature of the hot wall
$\overline{V}$	Dimensionless fluid velocity factor
X	Vertical axis (dimensionless)
Y	Horizontal axis (dimensionless)
α	Thermal diffusivity = $\kappa/\rho C_p$
β	Coefficient of volumetric expansion
δ_i^i	Kronecker Delta, = $\begin{matrix} 0 \text{ if } i \neq j \\ 1 \text{ if } i = 1 \end{matrix}$
θ	Dimensionless temperature
κ	Thermal conductivity
μ	Viscosity
ρ	Density
ν	Kinematic viscosity = μ/ρ

10. REFERENCES

(1) Balcomb, J.D., Hedstrom, J.C., and Moore, S.W., "Performance Data Evaluation of the Balcomb Solar Home," Los Alamos Scientific Lab Report No. LA-UR-79-2659 (1979).

(2) Bauman, F., Gadgil, A. Kammerud, R., and Greif, R., "Buoyancy-Driven Convection in Rectangular Enclosures: Experimental Results and Numerical Calculations," ASME paper No. 80-HT-66 presented at the 19th National Heat Transfer Conf., 27-30 July 1980, Orlando, Fla. (Lawrence Berkeley Laboratory Report LBL-10257).

(3) Buchberg, H., "Sensitivity of Room Thermal Response to Inside Radiation Exchange and Surface Conductance," Build. Sci., 6, 133 (1971).

(4) See the review article by S. Ostrach, "Natural Convection in Enclosures," Advanced Heat Transfer, 8, 161 (1972) and the papers cited therein.

(5) Rowley, F.B., Algren, A.B., Blackshaw, J.L., "Surface Conductances as Affected by Air Velocity, Temperature and Character of Surface," J. ASHVE, 2, 501 (1930).

(6) Rowley, F.B. and Eckley, W.A., "Surface Coefficients as Affected by Direction of Wind," J. ASHVE, 3, 870 (1931).

(7) ASHRAE Handbook of Fundamentals, Ch. 2 (1977).

(8) Nielsen, P.V., Ph.D. Thesis, "Flow in Air Conditioned Rooms," Technical University of Denmark (1974).

(9) Honma, H., Ph.D. Thesis, "Ventilation of Dwellings and Its Disturbances," Royal Institute of Technology, Stockholm, Sweden (1975).

(10) Weber, D.D., "Similitude Modeling of Natural Convection Heat Transfer Through an Aperture in Passive Solar Heated Buildings," Los Alamos Scientific Laboratory Report, LA-8385-T (1980).

(11) Wall, L.W., Dey, T., Gadgil, A.J., Lilly A.B. and Rosenfeld, A.H., "Conservation Options in Residential Energy Use: Studies Using the Computer Program TWOZONE," Lawrence Berkeley Laboratory Report LBL-5271 (August 1977).

(12) Roache, P.J., Computational Fluid Dynamics, Hermosa Publishers (1972).

(13) Spalding, D.B., "A Novel Finite Difference Formulation for Differential Expressions Involving Both First and Second Derivatives," Int'l J. Numerical Methods in Engrg., 4, 551-559 (1973).

(14) Runchal, A.K., "Convergence and Accuracy of Three Finite Difference Schemes for a Two-Dimensional Conduction and Convection Problem," Int'l J. Numerical Methods Engrg., 4, 541-550 (1973).

(15) Gadgil, A., Ph.D. Thesis, "On Convective Heat Transfer in Building Energy Analysis," Department of Physics, University of California, Berkeley (1980).

(16) Ruberg, K., Master's Thesis, "Heat Distribution of Natural Convection: A Modeling Procedure for Enclosed Spaces," Dept. of Architecture, Massachusetts Institute of Technology, Cambridge, MA. (1978).

(17) MacGregor, R.K. and Emery, A.F., "Free Convection Through Vertical Plane Layers--Moderate and High Prandtl Number Fluids," J. Heat Transfer, Trans. ASME, 91, 392-401 (1969).

(18) Raithby, G.D., Hollands, K.G.T., and Unny, T.E., "Analysis of Heat Transfer by Natural Convection Across Vertical Fluid Layers," J. Heat Transfer, Trans. ASME, 99, 287-293 (1977).

(19) El Sherbiny, S.M., Raithby, G.D., and Hollands, K.G.T., "Heat Transfer by Natural Convection Across Vertical and Inclined Air Layers," ASME Paper No. 80-HT-67, presented at the 19th National Heat Transfer Conf., 27-30 July 1980, Orlando, Fla.

(20) Shiralkar G., Gadgil A. and Tien, C.L., "High Rayleigh Number Convection in Shallow Enclosures with Different End Temperatures," submitted for publication to Int'l Journal of Heat and Mass Transfer.

(21) de Vahl Davis, G., "Laminar Natural Convection in an Enclosed Rectangular Cavity," Int'l J. Heat & Mass Transf., 11, 1675 (1968).

(22) Emery, A.F., "The Effect of a Magnetic Field Upon the Free Convection of a Conducting Fluid," J. Heat Transfer, Trans. ASME, 85, 2, 119-124 (1963).

(23) Portier, J.J. and Arnas, O.A., Heat Transfer and Turbulent Buoyant Convection, Vol. II, Hemisphere Publishing Corp., 1977, pp. 797-806.

(24) Burnay, G., Hannay, J., and Portier, J., Heat Transfer and Turbulent Buoyant Convection, Vol. II, Hemisphere Publishing Corp., 1977, pp. 807-811.

(25) Rubel, A., and Landis, R., "Numerical Study of Natural Convection in a Vertical Rectangular Enclosure," Phys. Fluids Suppl. II., 12, II-208 (1969).

(26) Quon, Charles, "High Rayleigh Number Convection in an Enclosure: A Numerical Study," Phys. Fluids, 12, 1, 12-19 (1972).

(27) Fromm, J.E., "A Numerical Method for Computing the Nonlinear, Time Dependent, Buoyant Circulation of Air in Rooms," National Bureau of Standards Building Science Series, 39, 1971, pp. 451-464.

(28) Carroll, W.L., Place, W., and Curtis, B., " A Passive Solar Residential Prototype for Energy Modeling," Lawrence Berkeley Laboratory Report LBL-10783 (1980), to be published.

(29) Sonderegger, R.C., Condon, P.E., and Modera, M.P., "In-Situ Measurements of Residential Energy Performance Using Electric Co-Heating," Lawrence Berkeley Laboratory Report LBL-10117 (1980).